ARTICLES

Photodegradation of Fluorescein in Solutions Containing *n*-Propyl Gallate

A. K. Gaigalas,* Lili Wang, K. D. Cole, and E. Humphries†

NIST, 100 Bureau Drive, Stop 8312, Gaithersburg, Maryland 20899-8312

Received: October 16, 2003; In Final Form: March 17, 2004

The frequency domain technique was applied to measure the effect of *n*-propyl gallate (nPG) on the apparent photodegradation rate of fluorescein in aqueous solutions. The illuminating light was modulated and the change in fluorescence from the illuminated region was detected synchronously. A constant flow rate was imposed on the fluorescein solution to control the mass transport of fluorescein into the illuminated region. The photodegradation response was described by a model which assumed two steps: (1) singlet oxygen production via energy transfer between the excited triplet state of fluorescein and molecular oxygen in the ground triplet state and (2) photodegradation via the interaction of fluorescein with singlet oxygen. It was assumed that nPG affects the photodegradation of fluorescein by quenching the oxygen singlet state. In the context of this model, the rate of singlet oxygen quenching by nPG was found to be $(1.3 \pm 0.2) \times 10^9$ $s^{-1}M^{-1}$. The product of the singlet oxygen photosensitization rate, k_{ox}, and the photodegradation rate, k_{pd}, was $k_{ox}k_{pd} = (0.60 \pm 0.3) \times 10^{17}$ s^{-2} M^{-2}. Photodegradation was observed in argon purged solutions and high concentrations of nPG, suggesting another photodegradation mechanism, such as direct electron transfer between fluorescein in the excited triplet state and fluorescein in the ground state. nPG also quenches the excited singlet state of fluorescein with a rate of $(2.5 \pm 0.3) \times 10^9$ s^{-1} M^{-1}.

Introduction

The photodegradation of fluorophore is an important issue in many biological assays, since both sensitivity and quantitation are affected adversely by the decay of the fluorescence signal.[1] Antifade agents have been developed to increase the photostability of the fluorescence signal.[2−5] The early work made some attempts to understand the action of the antifade agents; however a detailed picture was not presented. The time scale of the observed photodegradation is of the order of seconds and most likely is due to a combination of processes making it difficult to interpret. We have developed a frequency domain measurement technique which provides a convenient method for interpreting the role of antifade agents.[6] The frequency domain measurements have to be analyzed in terms of a mechanistic model, thus providing a link between observations and the underlying processes. The model has to be developed utilizing work with other techniques such as flash photolysis which are more suitable for elucidating the individual steps occurring during the photodegradation process.[7,8] Phenomenological parameters such as photodegradation quantum yield can be measured[9] and are very useful indicators of fluorophore photostability. However, they do not provide detailed links to the steps leading to photodegradation. The model of photodegradation can be constructed using information from many areas. Measurement of the highly reactive singlet oxygen production[10] showed that it was present in most fluorophore solutions exposed to light. Study of the photophysics of photosensitizer fluorophore, in the context of photodynamic therapy, showed that fluorophore exhibited substantial rates of singlet oxygen production and that the singlet oxygen could photodegrade the fluorophore itself.[11] Fluorophore photostability has also been studies in the context of laser applications.[12,13] In addition to singlet oxygen involvement,[14] specific models for triplet state reactions have been proposed.[15] The development of photofunctional materials requires attention to photodegradation.[16]

We apply the frequency domain technique to measure the apparent photodegradation rate of fluorescein with *n*-propyl gallate (nPG) added in solution. The compound nPG has been used to prolong the fluorescence response of labeled molecules observed by microscopy.[2,3] We start with a model of photodegradation, generalize some of the basic tenants of the measurement technique, and then present measurements and preliminary interpretations of the apparent photodegradation rate as a function of nPG concentration. The goal of this work is to demonstrate that the frequency domain technique is a useful tool for the study of antifade agents used to improve the photostability of fluorophore in biological assays.

A Matter of Nomenclature. The word "photodegradation" is used to describe the entire process which results in the decrease of fluorescence signal. The word "photodegradation" is also used to describe the specific reaction between fluorescein and photosensitized singlet oxygen. The context will determine which meaning of "photodegradation" is applicable.

Experimental Method

The apparatus which was used to carry out the frequency domain measurements has been described previously.[6] In

* Corresponding author. Telephone: (301) 975 2873. E-mail: adolfas.gaigalas@nist.gov.

† Present address: UMBC, Baltimore, MD.

10.1021/jp0371377
Published on Web 04/24/2004

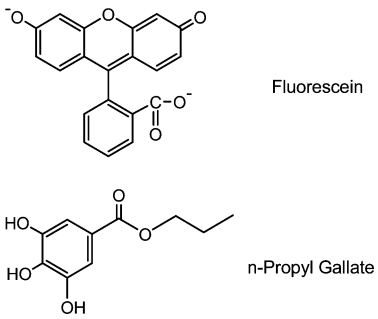

Figure 1. Structures of fluorescein dianion and *n*-propyl gallate. The fluorescein fluorescence originates from the intact three ring structure. A modification of any part of the three ring structure modifies the fluorescence at 512 nm. Fluorescence decreases if the oxygen on the three ring structure is protonated. Fluorescence disappears if any part of the three ring structure is broken or π bonding decreased.

summary, an argon ion laser operating at 488 nm was used to illuminate a solution of fluorescein flowing in a cuvette (47F-Q-10, Starna Cells, Inc.). (Certain commercial equipment, instruments, and materials are identified in this article to specify adequately the experimental procedure. In no case does such an identification imply recommendation and endorsement by the National Institute of Standards and Technology nor does it imply that the material and equipment is necessarily the best available for the purpose.) A mechanical chopper modulated the intensity of the illuminating laser beam, and the resulting fluorescence modulation was detected synchronously with a lock-in amplifier. The ratio of the quadrature and the in-phase components of the lock-in output was the primary measurement. The instrumental phase shift (ratio of quadrature to in-phase component) as a function of modulation frequency was measured by detecting the in-phase and quadrature signals from light scattered by a frosted glass plate placed in the cuvette. The instrumental phase shift was subtracted from that measured in fluorescein solutions.

A stock fluorescein solution was made by dissolving 55.96 mg of fluorescein powder (Molecular Probes Inc., MPR 71358, WO 18072) in 2.80 kg of 0.1 M borate buffer, pH = 9.0. The concentration of the fluorescein stock solution was 60.1 μM. All of the fluorescein solutions used in the photodegradation measurements were obtained by diluting the stock solution 100 fold in borate buffer. The fluorescein absorption coefficient at 488 nm was 87 000 L cm^{-1} mol^{-1}.[17] The optical density of a 1 cm thick slab of the fluorescein solution was less than 0.002. nPG (3,4,5-trihydroxybenzoic acid *n*-propyl ester) was obtained from Sigma Corp. (P-3130, M_r = 212.2 g/mol) and was used as received. The solution used in the photodegradation measurements was made by adding the gravimetrically determined amount of nPG powder and 2 mL of the fluorescein stock solution and mixing into 200 mL of borate buffer. The molecular structures of fluorescein and nPG are shown in Figure 1.

Model of Photodegradation. Photodegradation is assumed to occur via an interaction of the fluorophore in the ground singlet state with oxygen in the excited singlet state.[18] The concentration of the oxygen in the triplet (ground) and singlet (excited) states is given by $^3O_2$ and $^1O_2$, respectively. We assume that singlet oxygen is photosensitized via energy transfer reaction between the fluorophore and the oxygen in their respective triplet states. The quantum yield for singlet oxygen production by fluorescein in air saturated aqueous solutions is about 0.03[10] resulting in a significant concentration of singlet oxygen under conditions of high power illumination. The states involved in the process are shown in Figure 2. ^1N, $^1N^*$, ^3N, and ^XN denote the concentrations of fluorescein molecules in the ground state,

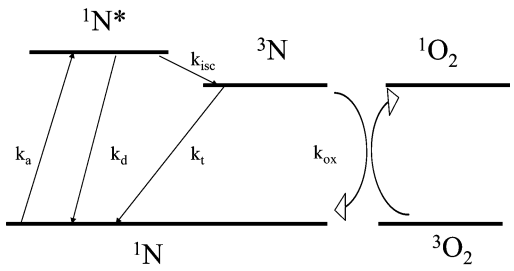

$$^3N + {}^3O_2 \xrightarrow{k_{ox}} {}^1N + {}^1O_2 \quad \text{photosensitization}$$

$$^1N + {}^1O_2 \xrightarrow{k_{pd}} {}^XN + {}^3O_2 \quad \text{photodegradation}$$

and

$$^1O_2 + G \xrightarrow{k_q} {}^3O_2 + G \quad \text{singlet quenching}$$

Figure 2. Schematic of the reaction scheme assumed for the analysis of data. *N* denotes the concentration of fluorescein in various states denoted by superscripts(notation adapted from[22]), *O* stands for concentration of oxygen, and *G* stands for the concentration of nPG. Singlet oxygen is produced via a photosensitization reaction. The singlet oxygen is depleted via two parallel reactions: the photodegradation of fluorescein and quenching by nPG.

^1S, the excited singlet state, $^1S^*$, the excited triplet state, ^3S, and the nonfluorescing photodegrade state, ^XS, respectively. The sum of the four concentrations is equal to $^1N^0$, the initial fluorophore concentration. In the case of varying illumination, the time variation of the populations of the three states can be modeled as[19]

$$\frac{d^1N^*}{dt} = k_a{}^1N - k_d{}^1N^* - k_{isc}{}^1N^* \quad \text{(a)}$$

$$\frac{d^3N}{dt} = k_{isc}{}^1N^* - k_t{}^3N - k_{ox}{}^3O_2{}^3N \quad \text{(b)}$$

$$\frac{d^1N}{dt} = k_d{}^1N^* + k_t{}^3N - k_a{}^1N + k_{ox}{}^3O_2{}^3N - k_{pd}{}^1O_2{}^1N \quad \text{(c)} \quad (1)$$

where the rate constants are defined in Figure 2. $^3O_2$ and $^1O_2$ are the concentrations of triplet (ground state) and singlet (excited state) oxygen. In eq 1a we have neglected stimulated emission, this is valid if the absorption rate is much smaller than the spontaneous decay rate.[20] The rate constant k_{pd} describes the photodegradation process

$$^1N + {}^1O_2 \xrightarrow{k_{pd}} {}^XN + {}^3O_2$$

and k_{ox} describes the photosensitization of singlet oxygen,

$$^3N + {}^3O_2 \xrightarrow{k_{ox}} {}^1N + {}^1O_2$$

Next we sum eq 1a−c and get

$$\frac{d}{dt}({}^1N^* + {}^3N + {}^1N) = -\frac{d^XN}{dt} = -k_{pd}{}^1O_2{}^1N \quad (2)$$

Equation 2 is relevant for the description of the photodegradation process. It models the decrease of the population of intact fluorophore. The time variation in eq 2 is that associated with the light modulation period (~0.1s). Equation 2 has to be solved

simultaneously with eq 1a and eq 1b. A very good approximate solution is obtained by taking the zero-order solutions of eq 1a and eq 1b (obtained by setting $d^1N^*/dt = 0$ and $d^3N/dt = 0$) and putting the resulting expressions into eq 2. The zero-order solution of eq 1a gives

$$^1N^* = \frac{k_a}{k_d + k_{isc}} {}^1N \tag{3}$$

which states that the population of the first excited singlet state is given by the ratio of photon absorption rate and the total decay rate. Similarly the zero-order solution of eq 1b gives

$$^3N = \frac{k_{isc}}{k_t + k_{ox}{}^3O_2} {}^1N^* = \frac{k_{isc}}{k_t + k_{ox}{}^3O_2} \frac{k_a}{k_d + k_{isc}} {}^1N \tag{4}$$

where we have used eq 3 to get the second part of the right side of eq 4. Substituting eq 3 and eq 4 into eq 2 gives the final result

$$\left[1 + \frac{k_a}{k_d + k_{isc}}\left(1 + \frac{k_{isc}}{k_t + k_{ox}{}^3O_2}\right)\right]\frac{d^1N}{dt} = -k_{pd}{}^1O_2{}^1N \tag{5}$$

In making the approximation, we assume that the photodegradation occurs from the ground-state interactions. The photon absorption and decay processes keep the excited-state populations in equilibrium with the ground-state population as given by the zero-order solutions to eq 1a and eq 1b.

We assume that nPG interacts with singlet oxygen resulting in the restoration of the triplet oxygen state (singlet quenching). The reactivity of singlet oxygen has been described by Turro[21] and Min.[22] The detailed pathway of the reaction between singlet oxygen and nPG is not known; however, it occurs only during illumination. Therefore, the time variation of singlet oxygen concentrations is given by

$$\frac{d^1O_2}{dt} = -k_{pd}{}^1N^1O_2 + k_{ox}{}^3N^3O_2 - k_qG^1O_2 - \gamma^1O_2$$

$$^3O_2{}^0 = {}^1O_2 + {}^3O_2 \tag{6}$$

Where $^3O_2{}^0$ is the concentration of triplet oxygen in the air saturated solution, G is the concentration of nPG, k_q is the rate of quenching of the oxygen singlet excited state by nPG, and γ is the rate constant representing all other processes that deplete singlet oxygen. The complete time dependence of the various concentrations is obtained by solving eqs 5 and 6.

We will write the absorption rate as $k_a = \sigma_a I_0$,[23] where σ_a (cm^2) is the molecular absorption cross section, and I_0 is the incident photon flux (1/s cm^2). During the experiment, we measure the total laser power P (W). The total power, P, can be converted into a photon flux, I_0, by dividing P by the cross sectional area of the laser beam and the energy per photon. Explicitly, $I_0 = P_cP$ where the conversion factor is given by $P_c = \lambda n/hcA_b$. Here λ is the wavelength, n is the index of refraction of the solution, h is Planck's constant, c is the speed of light in a vacuum, and A_b is the cross section area of the laser beam. This yields the result $k_a = \sigma_a P_c P$. Defining $k'_t = k_t + k_{ox}{}^3O_2{}^0$ and making the approximations $k_{isc} \ll k_d + k_a$, *and* $k_{isc} \gg k'_t$, eq 5 becomes

$$\frac{d^1N}{dt} = -\frac{k_{pd}}{1 + bP}{}^1O_2{}^1N \tag{7}$$

where we defined $b = (k_{isc}/k'_t)(P_c\sigma_a/k_d)$ (note $^3N \approx bP^1N$). To proceed further it is necessary to solve simultaneously eqs 6 and 7. As a first approximation, we linearize eq 7 by substituting $^1N^0$ for ^1N on the right and take the zero-order solution of eq 6

$$^1O_2 = \frac{k_{ox}{}^3O_2{}^0}{k_{pd}{}^1N^0 + k_qG + \gamma} {}^3N \tag{8}$$

Then eq 7 becomes

$$\frac{d^1N}{dt} = -\frac{k_X bP}{1 + bP}{}^1N \tag{9}$$

where k_X is defined as

$$k_X = k_{ox}{}^3O_2{}^0\frac{k_{pd}{}^1N^0}{k_{pd}{}^1N^0 + \gamma + k_qG} \tag{10}$$

where $^3O_2{}^0$ is the concentration of oxygen in the air saturated solution and $^1N^0$ is the initial fluorophore concentration. The apparent photodegradation rate, k_X, is a product of singlet photosensitization rate and the fraction of singlet oxygen decays which result in photodegradation. The form of eq 10 provides a specific dependence on G, the concentration of nPG.

Below we compare the measured values of the apparent photodegradation rate k_X to eq 10. The comparison is more meaningful if we normalize the apparent photodegradation rate by its value at zero nPG concentration.

Analysis of Data

The power of the modulated beam that illuminates the sample will be written as

$$P(t) = P_0 + \Delta P \cos(\omega t) \tag{11}$$

where P_0 is the constant component, ΔP is the amplitude of the modulated component, $w = 2\pi f$ is the radial modulation frequency, f is the frequency in Hz, and t is time. The kinetic model of photodegradation of the fluorophore will be extended to include flow. We assume that the flow will dominate all mass transport (diffusive and convective) into and out of the illuminating region and provide a well-defined initial concentration of fluorophore in the illuminated region. Equation 9 above is rewriten to describe a flowing solution

$$\frac{d^1N(x,t)}{dt} = -\frac{\eta P(t)}{1 + bP(t)}{}^1N(x,t) - \upsilon\frac{\partial^1N(x,t)}{\partial x} \tag{12}$$

where $\eta = k_X b$, υ is the flow velocity, and the last term in eq 12 gives the flow related flux of fluorophore in the illuminating region as a function of position. In principle we should also include transport terms for nPG and O_2; however the first term on the right in eq 12 already includes the approximation that uses only bulk concentrations on nPG and O_2. Figure 3 shows other simplifications inherent in writing eq 12. The laser beam in the flow cell has a circular cross section with a Gaussian intensity profile. The model uses a square cross section with uniform intensity distribution. The flow of fluorophore into the volume illuminated by the laser beam is assumed to be uniform over the top and bottom surfaces. The photodegradation depends on the intensity of incident light, consequently it will not be uniform over the illuminated volume. The model allows for a variable concentration of intact fluorophore in the illuminated region.

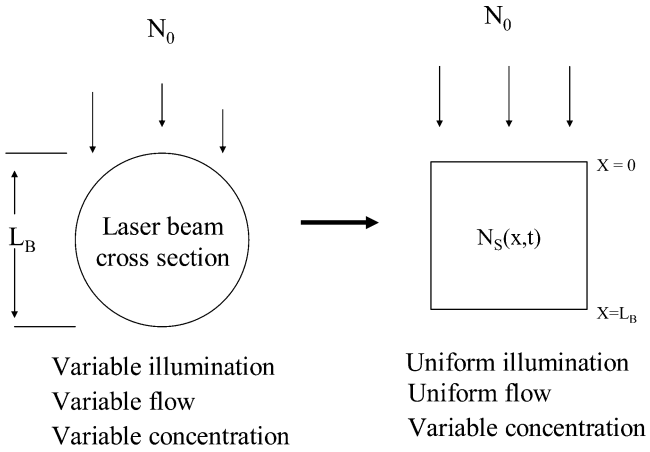

Figure 3. Diagram summarizing the simplifications inherent in the kinetic model which is used to analyze the frequency domain data. The circular laser beam is approximated by a square shape with uniform power density. The concentration of fluorescing species varies in a direction perpendicular to the laser beam. The flow is assumed to be uniform.

The measured fluorescence signal is given by eq 13 where we have used eq 3 to obtain the second term on the right side of eq 13.

$$F(t) = Ak_d\int_0^L {}^1N^*(x,t)\,dx = A\frac{k_d\sigma_a P_c}{k_d + k_{isc}}P(t)\int_0^L {}^1N(x,t)\,dx \tag{13}$$

Where A represents the characteristics of the optical measurement instrument, *P(t)* is the illuminating power given by eq 11, and ${}^1N(x,t)$ is the concentration of fluorophore given by the solution of eq 12. The fluorescence detector accepts signals from all parts of the illuminated region; therefore we need to integrate over this region in eq 12 to obtain the description of the observed signal.

$$\frac{d\int_0^L {}^1N(x,t)\,dx}{dt} = -\frac{\eta P(t)}{1 + bP(t)}\int_0^L {}^1N(x,t)\,dx - v\int_0^L \frac{\partial {}^1N(x,t)}{\partial x}dx \tag{14}$$

Defining the average observed signal as

$${}^1\bar{N}(t) = (1/L)\int_0^L {}^1N(x,t)\,dx$$

eq 14 becomes

$$\frac{d{}^1\bar{N}(t)}{dt} = -\frac{\eta P(t)}{1 + bP(t)}{}^1\bar{N}(t) - \frac{v}{L}({}^1N(L,t) - {}^1N(0,t)) \tag{15}$$

Equation 15 is the description of the observed fluorescence signal, where the second term on the right contains the concentration of fluorophore at the boundaries of the illuminated region. The value of concentration at the entrance to the illuminating region can be set equal to the concentration of fluorophore in solution, ${}^1N(0,t) = {}^1N^0$. The fluorophore concentration at the exit of the illuminated region can only be obtained by solving Eq 12. However, if the photodegradation rate is sufficiently small, then we can approximate the average signal as ${}^1\bar{N}(t) \approx ({}^1N^0 + {}^1N(L,t))/2$. With this approximation we get the equation of the previous paper[6]

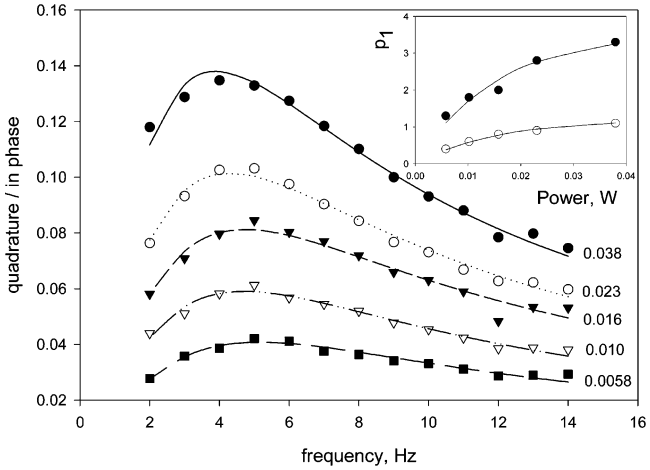

Figure 4. Discreet symbols show the response for several values of the incident laser power. The measurement errors, obtained from the standard deviation of repeated measurements of the lock-in amplifier response, are approximately the size of the symbols. The flow was held constant at 1.0 mL/min. The response grows with increasing power. The lines (solid, dotted, dashed, etc.) show the best fits to the data using eq 18. The inset shows the dependence of the parameter p_1 in eq 18 on the incident power. The values of p_1 are fit to an equation given by $p_1 = \eta P_0/(1 + bP_0)^2$, and the resulting parameter values are used to obtain the apparent photodegradation rate.

$$\frac{d{}^1\bar{N}(t)}{dt} = -\frac{\eta P(t)}{1 + bP(t)}{}^1\bar{N}(t) - \frac{2v}{L}({}^1\bar{N}(t) - {}^1N^0) \tag{16}$$

Another limiting case is where the fluorophores are photodegraded completely during transit of the laser beam. In this case ${}^1N(L,t) = 0$ and eq 15 becomes

$$\frac{d{}^1\bar{N}(t)}{dt} = -\frac{\eta P(t)}{1 + bP(t)}{}^1\bar{N}(t) + \frac{v}{L}{}^1N^0 \tag{17}$$

The fluorescence signal is calculated by substituting the assumed harmonic solution ΔN and eq 11 into either eq 16 or eq 17 and collecting terms proportionate to $e^{j\omega t}$. We get the final expression for the ratio of the quadrature component (proportionate to $je^{j\omega t}$) and the in-phase component (proportionate to $e^{j\omega t}$) of the detected fluorescence signal,

$$\frac{\text{quadrature}}{\text{in-phase}} = \frac{p_1\omega}{p_2 + \omega^2} \tag{18}$$

where $p_1 = \eta P_0/(1 + bP_0)^2$ while the parameter p_2 differs for eqs 16 and 17. From the definition of b and η, we note that the ratio η/b is just the photodegradation rate k_X. The functional form of the ratio in eq 18 comes directly from eq 15 assuming harmonic solutions for both ${}^1\bar{N}(t)$ and ${}^1N(L,t)$. While the functional form of p_1 is always as given above, the value of the parameter p_2 depends on the properties of ${}^1N(L,t)$ and indirectly on beam focusing and flow velocity.

Results and Discussion

Equation 18 gives the prediction of the dependence of the ratio on modulation frequency in the context of the model discussed above. Below we discuss the measured results in solutions of fluorescein with varying concentrations of nPG. Figure 4 shows the dependence of the ratio of the quadrature

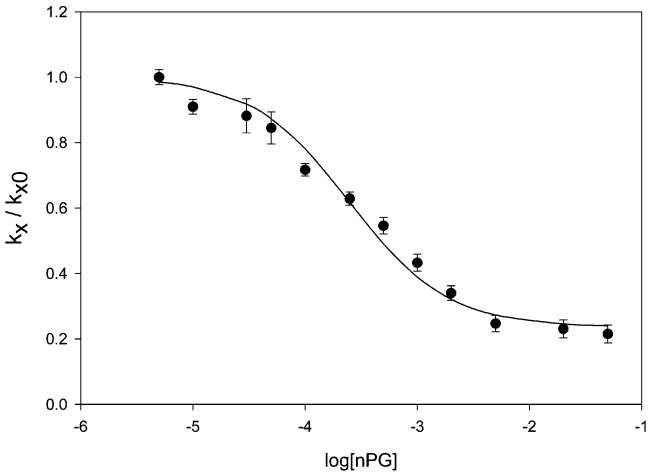

Figure 5. Solid circles represent the ratio of the apparent photodegradation rate at a given concentration of nPG to the apparent photodegradation rate in the absence of nPG. The errors were obtained from the standard deviation of results from repeated measurements. All of the apparent photodegradation rates were obtained as specified in Figure 4. The fluorescein concentration was 0.6 μM, pH = 9, and the solution was saturated with air. The solid line is a fit to the model discussed in the text.

TABLE 1: Measured Values of Apparent Photodegradation Rate, k_X (s^{-1})

	solution conditions		
nPG concn	0.6 μM fluorescein + 0.2mM O_2	0.6 μM fluorescein	1.2 μM fluorescein + 0.2 mM O_2
0 μM	87 ± 4	55 ± 8	108 ± 8
10 μM	81 ± 8	35 ± 8	99 ± 8
5 mM	20 ± 8	14 ± 8	39 ± 8

and in-phase components of the modulated fluorescence signal on modulation frequency for different values of incident laser power. The concentration of nPG was 100 μM, and the flow rate was set to 1.0 mL/min. Each of the curves in Figure 4 is for a different incident laser power, and the power varied by about a factor of 10. The continuous lines in Figure 4 correspond to the best fits to eq 18. According to the definition of the parameters in eq 18, $p_1 = \eta P_0/(1 + bP_0)^2$ where $\eta = k_X b$. Thus k_X can be obtained from the ratio of the two parameters which describe the dependence of the value of p_1 on power. The procedure was followed for a range of concentrations of nPG. Some of the results are shown in Table 1 for extreme values of nPG concentrations, as well as different concentrations of molecular oxygen and fluorescein. The errors are obtained from the variation of results from repeated measurements. The results for saturated solutions are somewhat larger than those reported in the previous work.[6] The difference is most likely due to a larger averaging over flow velocities in the previous work (the beam was less focused). The expected photodegradation quantum yield, ϕ_{pd}, can be estimated from the parameters in the model $\phi_{pd} = (d^1N/dt)/k_a{}^1N \approx k_X k_{isc}/k_d k_t \approx 100 k_X \tau$ where τ is the observed lifetime. Therefore the values of k_X in Table 1 can be used to obtain relative photodegradation quantum yields which are of the order of 10^{-5}. Photodegradation measurement have been reported for fluorescein derivatives in an oxygen free environment (ethanol solutions).[24] The reported photodegradation quantum yield was of the order 10^{-5}.

Figure 5 shows the ratio of the apparent photodegradation rate at a given concentration of nPG to the apparent photodegradation rate in the absence of nPG. The solution was saturated with air. The apparent photodegradation rate decreases significantly in the presence of nPG. However, a significant level of photodegradation remains even at high concentrations of nPG. The data in Figure 5 are discussed in the framework of the model described above which assumes that the photodegradation occurs via reaction of fluorescein with photosensitized singlet oxygen. The prediction of the model is given by eq 10 which can be used to form the ratio of apparent photodegradation rates

$$\frac{k_X(G)}{k_X(0)} = \frac{1}{1 + \dfrac{k_q}{k_{pd}{}^1N^0 + \gamma}G} \tag{19}$$

Contrary to the results shown in Figure 5, eq 19 predicts that at large concentrations of nPG the apparent photodegradation rate will vanish. We assume that the nPG independent photodegradation can be modeled by adding a constant term to the right side in eq 19. Calling this constant term "bkg", we fit the data in Figure 5 to a function of the form $(1 - \text{bkg})/(1 + aG) + \text{bkg}$ obtaining a value of 4010 ± 580 M^{-1} for the factor multiplying G in eq 19.

$$\frac{k_q}{k_{pd}{}^1N^0 + \gamma} = 4010\ M^{-1} \tag{20}$$

The initial fluorescein concentration, $^1N^0$, is known to be 0.6 μM. The lifetime of singlet oxygen in water is about 3μs[25,26] and provides an estimate of $\gamma = {}^1/_3\ \mu s = 3.3 \times 10^5\ s^{-1}$. Assuming that the photodegradation rate constant has a diffusion limited[27] value of the order $10^9\ s^{-1}\ M^{-1}$, we get an upper estimate of 10^3 for the factor $k_{pd}{}^1N^0$ which is much smaller than γ. Therefore the photodegradation contribution in eq 20 can be neglected giving an estimate of the oxygen singlet quenching rate by nPG, $k_q = 4010\gamma = (1.3 \pm 0.2) \times 10^9\ s^{-1}\ M^{-1}$. This value is close to that of a diffusion controlled reaction.

Equation 10 gives the relationship between the apparent photodegradation rate and parameters in the model. For the case of zero nPG concentration and neglecting the photodegradation contribution in the denominator of eq 10, we get the relation

$$k_X = k_{ox}{}^3O_2{}^0\frac{k_{pd}{}^1N^0}{\gamma} \tag{21}$$

The data in Table 1 for zero nPG concentration provides estimates of the slope of the linear dependence of k_X on the concentration of fluorescein or oxygen. The two values of the slope divided by the appropriate concentration and multiplied by γ give the result $k_{ox}k_{pd} = (0.5 \pm 0.2) \times 10^{17}\ s^{-2}\ M^{-2}$ for a change in fluorescein concentration and $k_{ox}k_{pd} = (0.7 \pm 0.3) \times 10^{17}\ s^{-2}\ M^{-2}$ for a change in oxygen concentration. Similar numbers are obtained using the values in Table 1 for an nPG concentration of 10 μM. In the context of the model we can evaluate only the product of the singlet oxygen photosensitization rate, k_{ox}, and the photodegradation rate, k_{pd}. Combining the above results we get the best estimate of the product $k_{ox}k_{pd} = (0.60 \pm 0.3) \times 10^{17}\ s^{-2}\ M^{-2}$ which is about an order of magnitude smaller than if both reactions were diffusion controlled.

The data in the second and third columns of Table 1 were formed into ratios and plotted in Figure 6. The continuous line in Figure 6 reproduces the trend of the ratio in air saturated solutions shown in Figure 5. The solid circles in Figure 6 show the measured ratios when the concentration of fluorescein is increased 2-fold in air saturated solutions (third column of Table 1). The k_{X0} in the ratio corresponds to concentrated fluorescein

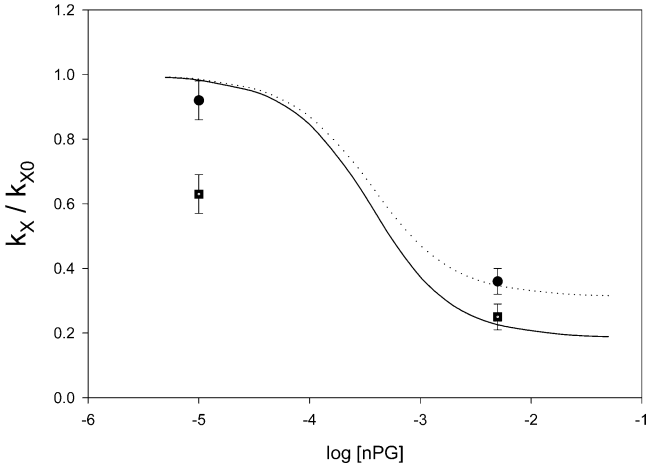

Figure 6. Solid squares show the ratio of k_X at a given concentration of nPG to k_X in the absence of nPG in argon purged solutions. The errors were obtained from the standard deviation of results from repeated measurements. As shown in Table 1, the values of k_X are smaller; however there is still a significant dependence on the concentration of nPG. The solid circles show the ratio in solutions with a fluorescein concentration of 1.2 μM and saturated with air. The absolute values of k_X increase, but the ratio follows the same dependence as in Figure 5. The ratio at large nPG concentrations is somewhat larger.

in air saturated solutions without nPG. Except for an increase in the parameter "bkg", the ratio follows the model as indicated by the dotted line in Figure 6. These observations suggest that the photodegradation at high nPG concentrations, where singlet oxygen is completely quenched, depends on fluorescein concentration and thus is likely due to interaction between fluorescein molecules. The absolute value of k_X increased from 87 ± 4 s^{-1} at 0.6 μM fluorescein to 108 ± 8 s^{-1} at 1.2 μM fluorescein (no nPG). Measurements were made in purged solutions of fluorescein. The value of k_X decreased from 87 ± 4 s^{-1} in air saturated 0.6 μM fluorescein solution to 55 ± 8 s^{-1} in argon purged 0.6 μM fluorescein solution (no nPG). The ratios (from column 2 in Table 1) are shown by the solid square symbols in Figure 6 where the denominator in the ratio is k_{X0} for fluorescein in argon purged solutions without nPG. The ratio is largely independent of oxygen concentration at high values of nPG concentration. The significant dependence of the ratio at low concentration of nPG in argon purged solutions suggests that there may be an additional nPG dependent photodegradation process which most likely is due to direct interaction of fluorescein with nPG. Figure 7 shows the fluorescence intensity and fluorescence lifetime dependence on nPG concentration. The fact that the intensity and lifetime change in the same manner indicates that the fluorescence quenching is due to nPG interaction with fluorescein in the excited $^1S^*$ state (dynamic quenching). The quenching constant of 10.7 ± 0.8 M^{-1} and the unperturbed lifetime of fluorescein (4.3×10^{-9} s) yield a collisional quenching rate of $(2.5 \pm 0.3) \times 10^9$ s^{-1} M^{-1}.[28] This value is of the order expected for purely diffusion controlled quenching. Thus nPG provides an alternate relaxation path for the $^1S^*$ excited state of fluorescein. We neglect possible quenching of the $^1S^*$ by other fluorescein molecules.[29] It is likely that a similar interaction takes place between nPG and fluorescein in the excited triplet state, ^3S. Thus nPG will reduce photodegradation in argon purged solutions of fluorescein by quenching the excited singlet and triplet states of fluorescein and reducing the amount of reactions involving the triplet state. However at this time it is not clear what those reactions may be in argon purged solutions of fluorescein. The direct interaction between nPG and fluorescein was not included in the previous model where it was assumed that nPG interacts only with singlet oxygen. The data in Figure 6 suggest that the ratio, k_X/k_{X0}, can be represented by a surface in the multidimensional space spanned by the concentrations of all of the species involved in the process. An extended model should provide a representation of this surface together with estimates of the relevant rate constants.

Finally we speculate on the nature of the photodegradation process which does not depend on the presence of nPG or oxygen. Photoinduced electron transfer (ET) and the formation of ion pairs have been studied extensively.[30,31] Direct ET between excited fluorescein and an acceptor has been reported.[32] Photoinduced ET in eosin, a compound related to fluorescein, has been reported[33] and correlated with photodegradation of eosin. Therefore it is likely that fluorescein in the triplet excited state, ^3S, can undergo electron transfer reactions with fluorescein

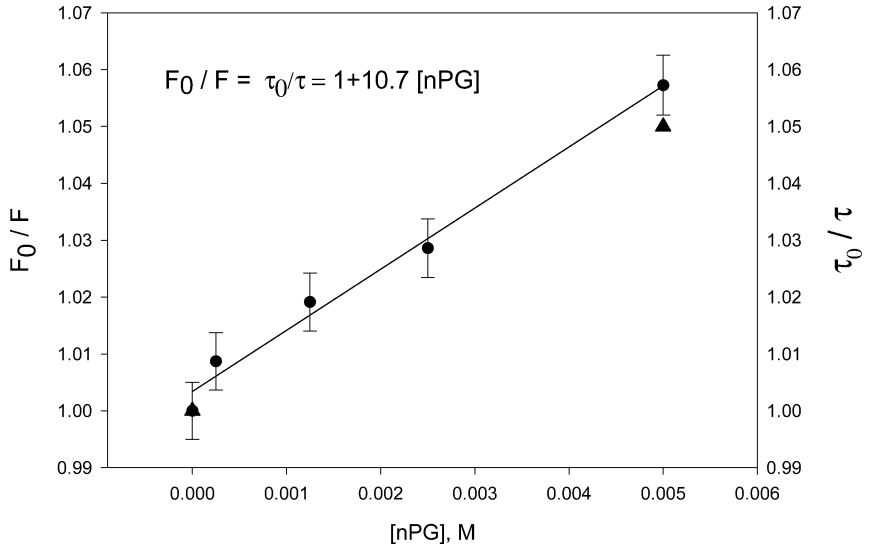

Figure 7. Solid circles show the fluorescence intensity quenching by nPG. The errors were obtained from the standard deviation of results from repeated measurements. The left axis shows the ratio of fluorescence intensity in the absence of nPG to the intensity at a given concentration of nPG. The right-hand axis shows the corresponding ratio of measured fluorescence lifetimes denoted by solid triangles. The concentration of fluorescein was 0.6 μM. The data suggest that nPG is a source of dynamic quenching by providing another path for de-excitation of the $^1S^*$ excited state of fluorescein.

in the singlet ground state, ^1S, and initiate a photodegradation pathway.[19] The ET mechanism is not expected to have significant dependence on the concentration of nPG and thus could be responsible for the observed photodegradation at high nPG concentrations. The exchange of protons between excited fluorescein molecules and buffer is unlikely in borate buffer.[34]

Conclusion

We have applied the frequency domain technique to the measurement of the apparent photodegradation rate of fluorescein in aqueous solutions with varying concentrations of nPG. The photodegradation rate decreased significantly with increasing nPG concentration. This behavior was rationalized by assuming that the nPG quenches the singlet oxygen state, thus preventing its interaction with the fluorescein molecule. Singlet oxygen is produced by energy transfer between the triplet states of the excited fluorescein and molecular oxygen in the triplet ground state. The above scenario was incorporated into a model. In the context of the model, the rate of singlet oxygen quenching by nPG was found to be $(1.3 \pm 0.2) \times 10^9$ s^{-1} M^{-1}. Measurement in argon purged solutions yielded reduced but significant photodegradation rates even at high nPG concentrations. A possible mechanism of photodegradation at high concentrations of nPG may be electron transfer (ET) between the ground state singlet and excited triplet state of fluorescein molecules. The ET transition is expected to be independent of nPG. The dependence of the photodegradation rate on nPG concentration in argon purged solutions was rationalized by invoking quenching of the singlet and triplet excited states of fluorescein by nPG.

The description of the photodegradation of fluorescein in aqueous solutions containing oxygen and nPG starts with the excitation of the triplet state of fluorescein and then branches out into a set of parallel reaction pathways resulting in fluorescein photodegradation. Clearly the model needs to be expanded to include this complexity. We are planning on improvements to the apparatus to allow measurement of higher harmonics and to extend the measurements and model to additional fluorophore and antifade (stabilizing) agents.

References and Notes

(1) Tsien, R. Y.; Waggoner, A. Fluorophores for confocal microscopy: photophysics and photochemsitry. In *Handbook of Confocal Microscopy*; Pawley, J., Ed.; Plenum Press: New York, 1994.

(2) Johnson, G. D.; Davidson, R. S.; McNamee, K. C.; Russell, G.; Goodwin, D.; Holborow, E. J. *J. Immunol. Methods* **1982**, *55*, 231.

(3) Giloh, H.; Sedat, J. W. *Science* **1982**, *217*, 1252.

(4) Bock, G.; Hilchenbach, M.; Schauenstein, K.; Wick, G. *J. Histochem. Cytochem.* **1985**, *33*, 699.

(5) Picciolo, G. L.; Kaplan, D. S. *Adv. Appl. Microbiol.* **1984**, *30*, 197.

(6) Gaigalas, A. K.; Wang, L.; Robert F. Vogt, J. *Photochem. Photobiol.* **2002**, *76*, 22.

(7) Porter, L. G. *Chemistry in Microtime*; Imperial College Press: London, 1997.

(8) Rabek, J. F. *Experimental Methods in Photochemistry and Photophysics*; John Wiley and Sons: Chichester, 1982.

(9) White, J. C.; Stryer, L. *Anal. Biochem.* **1987**, *26*, 442.

(10) Gandin, E.; Lion, Y.; Vorst, A. V. d. *Photochem. Photobiol.* **1983**, *37*, 271.

(11) Bergh, H. v. d. *Seminars in Ophthalmology* **2001**, *16*, 181.

(12) Mackey, M. S.; Sisk, W. N. *Dyes Pigm.* **2001**, *51*, 79.

(13) Jones, G., III Photochemistry of Laser Dyes. In *Dye Laser Principles With Applications*; Duarte, F. J., Hillman, L. W., Eds.; Academic Press: Boston, 1990; p 287.

(14) Stracke, F.; Heupel, M.; Thiel, E. *J. Photochem. Photobiol., A* **1999**, *126*, 51.

(15) Becker, S.; Gregor, I.; Thiel, E. *Chem. Phys. Lett.* **1998**, *283*, 350.

(16) Horiuchi, T.; Miura, H.; Uchida, S. *Chem. Commun.* **2003**, 3036.

(17) DeRose, P. C.; Kramer, G. W. In preparation.

(18) Song, L. L.; Varma, C.; Verhoeven, J. W.; Tanke, H. J. *Biophys. J.* **1996**, *70*, 2959.

(19) Song, L.; Hennink, E. J.; Young, I. T.; Tanke, H. J. *Biophys. J.* **1995**, *68*, 2588.

(20) Loudon, R. *The Quantum Theory of Light*, 3rd ed.; Oxford University Press: New York, 2000.

(21) Turro, N. J. *Modern Molecular Photochemistry*; University Science Books: Sausalito, CA, 1991.

(22) Min, D. B.; Boff, J. M. *Compr. Rev. Food Sci. Food Saf.* **2002**, *1*, 58.

(23) Milonni, P. W.; Eberly, J. H. *Lasers*; Wiley: New York, 1988.

(24) Meallier, P.; Guittonneau, S.; Emmelin, C.; Konstantinova, T. *Dyes Pigm.* **1999**, *40*, 95.

(25) Parker, J. G.; Stanbro, W. D. *J. Photochem.* **1984**, *25*, 545.

(26) Dedic, R.; Svoboda, A.; Psencik, J.; Lupinkova, L.; Komenda, J.; Hala, J. *J. Lumin.* **2003**, *102*−*103*, 313.

(27) Steinfeld, J. I.; Francisco, J. S.; Hase, W. L. *Chemical Kinetics and Dynamics*; Prentice Hall: Englewood Cliffs, NJ, 1989.

(28) Lakowicz, J. R. *Principles of Fluorescence Spectroscopy*, 2nd ed.; Kluwer Academic/Plenum Publishers: New York, 1999.

(29) Plant, A. L. *Photochem. Photobiol.* **1986**, *44*, 453.

(30) Weller, A. *Zeitschrift fur Physikalische Chemie, Neue Folge* **1982**, *133*, 93.

(31) Gould, I. R.; Young, R. H.; Mueller, L. J.; Farid, S. *J. Am. Chem. Soc.* **1994**, *116*, 8176.

(32) Goetz, M.; Hess, S.; Beste, G.; Skerra, A.; Michel-Beyerle, M. E. *Biochemistry* **2002**, *41*, 4156.

(33) Ohno, T.; Kato, S.; Koizumi, M. *Bull. Chem. Soc. Jpn.* **1966**, *39*, 232.

(34) Alvarez-Pez, J. M.; Ballesteros, L.; Talavera, E.; Yguerabide, J. *J. of Phys. Chem. A* **2001**, *105*, 6320.